Change in the Proton T_1 of Fat and Water in Mixture

Houchun H. Hu[*] and **Krishna S. Nayak**
Magnetic Resonance Engineering Laboratory, Signal and Image Processing Institute, Ming Hsieh Department of Electrical Engineering, University of Southern California, Los Angeles, California, USA

Abstract

This work describes observed changes in the proton T_1 relaxation time of both water and lipid when they are in relatively homogeneous mixtures. Results obtained from vegetable oil–water emulsions, pork kidney and lard mixtures, and excised samples of white and brown adipose tissues are presented to demonstrate this change in T_1 as a function of mixture fat fraction. As an initial proof of concept, a simpler acetone-water experiment was performed to take advantage of complete miscibility between acetone and water and both components' single chemical shift peaks. Single-voxel MR spectroscopy was used to measure the T_1 of predominant methylene spins in fat and the T_1 of water spins in each setup. In the vegetable oil–water emulsions, the T_1 of fat varied by as much as 3-fold when water was the dominant mixture component. The T_1 of pure lard increased by 170 msec (+37%) when it was blended with lean kidney tissue in a 16% fatty mixture. The fat T_1 of lipid-rich white adipose tissue was 312 msec. In contrast, the fat T_1 of leaner brown adipose tissue (fat fraction 53%) was 460 msec. A change in the water T_1 from that of pure water was also observed in the experiments.

Keywords

fat; water; T_1 relaxation; T_1 bias; T_1 relaxation in mixture

Several reports have recently described robust chemical-shift fat-water separation methods in MRI (1–4). Fat quantification studies utilizing some of these techniques have been described in assessing hepatic steatosis (5), epicardial fat (6), and total body fat composition in obesity research (7). With methods such as the iterative decomposition of water and fat with echo asymmetry and least-squares estimation (IDEAL) approach (2), a fat-signal fraction is typically computed on a voxel-by-voxel basis as $F/(F + W)$, where F and W denote the decomposed fat and water signals, respectively. In order for the fat-signal fraction to accurately represent the underlying fat content, several works have shown that it is important to consider a multipeak rather than a single-peak spectral model for fat (8,9), T_2^* weighting (8,10), and T_1 and noise bias between F and W signals (8,11). To specifically minimize T_1-bias between fat and water spins, the use of small flip angles (≈5°) in IDEAL spoiled-gradient-echo imaging has been suggested (11). In addition to the fat-signal fraction, a fat-only signal fraction (F/F_{PURE}) has also been reported, where F_{PURE} is the signal from a separate reference voxel containing pure fat (12). This work specifically investigates deviation in the proton T_1 spin-lattice relaxation rate of fat from its pure natural T_1 value when fat is present in relatively homogeneous mixtures. Thus, it is hypothesized that the F/F_{PURE} ratio may also be susceptible to T_1-bias. Results from several phantoms constructed of acetone-water mixtures, oil-water emulsions, kidney-lard mixtures, and excised white and brown adipose tissue samples from mice are presented to corroborate this hypothesis. Although the change in the T_1 of the methylene fat moiety is the

*Correspondence to: Houchun H. Hu, University of Southern California, Ming Hsieh Department of Electrical Engineering, 3740 McClintock Avenue, EEB 408, Los Angeles, CA 90089–2564. houchunh@usc.edu.

primary focus in this article, we also demonstrate the change in the proton T_1 of water (and acetone).

MATERIALS AND METHODS

T_1 Measurements

All experiments were performed at room temperature on a General Electric 3-T scanner (Signa HD 12M5; GE Healthcare, Waukesha, WI). We used single-voxel proton MR spectroscopy (point-resolved MRS) (13) for both accurate spectral separation of chemical moieties and T_1 measurements. Data were acquired with a wrist coil (BC-10; Mayo Clinic, Rochester, MN). After Fourier transformation of the acquired free-induction-decay signal, baseline and phase correction were performed. Subsequently, the area under each spectral peak of interest was computed. Analysis was performed with the Java-based magnetic resonance user interface (MRUI) software (http:/sermn02.uab.cat/mrui/) (14,15), where the user can specify the number of spectral peaks to be fitted. Signal integrals were quantified for the water peak (near 4.7 ppm) and only the primary methylene (—CH_2—)$_n$ fat peak (near 1.3 ppm). For the acetone-water setup, the acetone peak was quantified (near 2.4 ppm downfield from water) in place of fat. Scan parameters for MRS were echo time = 23 msec, $20 \times 20 \times 20 mm^3$ voxel, 2048 data points, 2.5- kHz bandwidth, no water suppression, and at least eight signal averages. In each experiment, the pulse repetition time (TR) was varied while all other parameters were held constant. The specific TR values used in each experiment are listed in Table 1. We used different TR values to ensure adequate sensitivity in measuring the anticipated T_1 values. After spectral peak quantification, the T_1 relaxation rates of acetone/water/methylene fat were estimated with least-squares curve-fitting routines in Matlab (The MathWorks, Natick, MA). The computed areas under each spectral peak were plotted vs TR, and a monoexponential saturation-recovery equation $S_{TR} = S_O(1 - \exp(-TR/T_1))$ was used for fitting. S_{TR} is the integrated peak spectral area for a given TR, and S_O is the equilibrium value (weighted by constant T_2 relaxation). No numerical constraint was placed on the estimated T_1 values during data fitting. The procedures were similar to those used by Sharma et al. (16).

Acetone-Water Mixtures

As an initial proof of concept, we substituted fat with acetone. Mixtures of acetone (Alfa Aesar, Ward Hill, MA) and un-doped distilled water were prepared in 20% increments by volume in 50-mL vials. Acetone was used for convenience due to its complete miscibility with water. Furthermore, unlike fat, acetone is characterized by a true *single* chemical shift peak (2.3 ppm), as shown in Fig. 1. MRS measurements were acquired separately for each mixture of acetone and water. We hypothesized that the component T_1 values of acetone and water would change as a function of mixture composition.

Oil-Water Emulsions

Homogeneous emulsions consisting of vegetable (corn) oil and distilled water were prepared (Fig. 2a) in 60-mL bottles, similar to the setup described previously by Bernard et al. (17). Agar gel (2% by weight) and dioctyl sulfosuccinate sodium salt (Alfa Aesar) were used to stabilize the emulsions. No contrast agent or additional chemicals were added to the water. The emulsions were prepared slowly over a heat-stir plate and subsequently cooled to allow the mixture to stay intact. As the photograph in Fig. 2a shows, the oil and water suspensions are homogeneous and stable. MRS measurements were collected on a subset of the mixtures (10%, 30%, 60%, and 80% fat by volume). We similarly hypothesized that the component T_1 values of fat and water would change as a function of mixture composition.

Pork Kidney–Lard Mixtures

Fresh pork kidney and lard (Farmer John, Los Angeles, CA) were purchased from a local market. The kidney was cut into three portions and was initially devoid of any fat tissue (Fig. 4a). In part I, the tissue was left unaltered. In part II, the tissue was thoroughly homogenized in a blender. In part III, the tissue was additionally mixed with melted lard and further homogenized in a blender. The resulting purée-like mixture had a fat fraction of about 16%, as subsequently determined by MRS. MRS measurements were collected separately for each of the three portions and for pure lard. We hypothesized that the T_1 of water (kidney) would not change between parts I and II as a result of homogenization. We additionally hypothesized that the T_1 of lard would change in part III from that of pure lard.

White vs Brown Adipose Tissue

Excised samples of white and brown adipose tissues were obtained from mice (Fig. 5a). Whereas white adipose tissue is primarily a lipid storage reservoir, brown adipose tissue is involved in energy expenditure and thermogenesis (18). White and brown adipocytes represent two naturally occurring physiologic tissues that have distinct differences in intracellular fat content. Due to its higher metabolic activity, the fat fraction of brown adipose tissue has been shown to be lower than that of white adipose tissue (19). Under light microscopy, brown adipocytes are characterized by numerous small intracellular lipid droplets that are surrounded by an abundance of intracellular water. In contrast, white adipocytes contain only a single large lipid micelle and have very little additional intracellular space. The chemical composition of triglycerides in brown and white adipose tissue is not significantly different (20). We performed MRS measurements on one sample of white adipose tissue and two samples of brown adipose tissue with different fat fractions. We hypothesized that the T_1 of fat and water in white and brown adipose tissue would differ.

RESULTS

Acetone-Water Mixtures

Figure 1 summarizes results from the acetone-water mixtures. Raw, unprocessed MRS spectra obtained from the 60% acetone mixture are shown in Fig. 1a in units of ppm. Spectra obtained with the shortest (dashed black) and longest TRs (solid black) are highlighted. The effect of saturation recovery as a function of TR is clearly evident. Figure 1b plots the integrated spectral signals as a function of TR for acetone and water. The measured data points and fitted curves suggest excellent agreement with the theoretical T_1 saturation-recovery signal model. The estimated component T_1s of acetone and water are indicated. Figure 1c illustrates the evident change in both the T_1 of acetone and water as a function of acetone volume fraction. Pure water (0%) had a T_1 of 2.7 sec, whereas pure acetone (100%) had a longer T_1 of 4.1 sec. Across the mixtures, water T_1 changed by approximately 32%, while acetone T_1 varied by approximately 28%. Note that the component *water* T_1 approaches the pure T_1 of *acetone* as the acetone volume fraction nears 100% (e.g., mixture is acetone dominant). Similarly, the component *acetone* T_1 approaches the pure T_1 of *water* as the acetone volume fraction nears 0% (e.g., mixture is water dominant).

Oil-Water Emulsions

Figures 2 and 3 summarize results from the oil-water emulsions. A photograph of the homogenized suspensions is shown in Fig. 2a. Data are presented in a similar format to Fig. 1. Raw, unprocessed MRS spectra from 10% and 60% fat emulsions are shown in Fig. 2b and c, respectively. In Fig. 2d, fitted data curves for the water components are shown. Similarly, in Fig. 2e, fitted data curves for the fat components are plotted. The data curves in Fig. 2e have been scaled individually to facilitate plotting in the same figure. Figure 3 illustrates the change

in both the T_1 of fat and water as a function of mixture fat fraction. The largest observed change in fat T_1 from its pure value is more than 3-fold, while the largest variation in water T_1 is approximately 59% of its pure value. A similar trend is observed in comparison to Fig. 1c. The component *water* T_1 approaches the pure T_1 of *fat* as the fat volume fraction nears 100% (e.g., mixture is fat dominant). Likewise, the component *fat* T_1 approaches the pure T_1 of *water* as the fat volume fraction nears 0% (e.g., mixture is water dominant). Whereas acetone was the *longer* T_1 moiety in the previous experimental setup, water molecules were the *longer* T_1 species in the oil-water emulsions. Interestingly, note that the shape of the acetone data points in Fig. 1c (squares) and those of water (open circles) in Fig. 3 behave similarly as a function of mixture composition, albeit in a mirrored manner.

Pork Kidney–Lard Mixtures

Figure 4a shows a photograph of the three different kidney/lard preparations. Figure 4b shows the corresponding MRS spectra. The fat peak (at 1.3 ppm) and the 16% fat fraction in part III from melted lard are clearly noticeable in the spectrum. The spectra also show that parts I and II are devoid of any fat species. Figure 4c plots the integrated signals for the water component in parts I, II, and III. As anticipated, homogenizing the kidney (part II) did not affect the T_1 of the water component relative to intact kidney tissues (part I). There is a slight decrease in the water T_1 of about 34 msec (5% change) when kidney tissues were homogenized with lard (part III). This change is insignificant in comparison to the variation observed in the associated lard T_1. Figure 4d plots similar curves for the lard component between pure lard and mixed lard in part III. The measured T_1 of lard in part III (black squares) represents a significant 37% increase (282 to 451 msec) over the T_1 of pure lard (open squares). The data curve for pure lard in Fig. 4d has been scaled down 5-fold to facilitate plotting in the same figure.

White vs Brown Adipose Tissue

Figure 5 summarizes results from the experiment using excised white and brown adipose tissue from mice. Figure 5a shows representative MRS spectra of the two tissues. Note that white adipose tissue is predominantly composed of lipids, whereas brown adipose tissue contains an appreciable amount of water signal at around 4.7 ppm. Figure 5b plots the integrated signals for the water components of two samples of brown adipose tissue with different fat fractions. The leaner sample with a 53% fat fraction had a water T_1 of 1087 msec (gray squares), while the fattier sample with a fat fraction of 83% had a shorter water T_1 of 890 msec (black squares). Figure 5c shows corresponding plots for the fat components. Note that white adipose tissue had a fat T_1 of 312 msec, consistent with previous literature findings in vivo (21,22). However, the fat T_1 increased as the fat fraction decreased. The fat T_1 of the 83% brown adipose tissue was 341 msec, while the fat T_1 of the 53% sample was 460 msec.

DISCUSSION AND CONCLUSION

We have demonstrated the phenomenon of change in the T_1 of both fat and water moieties from their pure T_1 values when they are present in relatively homogeneous mixtures. Fat and water are naturally immiscible and a mixture of the two can only be treated as a suspension. Acetone and water are, however, completely miscible, and results from the proof-of-concept acetone-water experiment provided compelling evidence of the T_1 effect investigated in this work. For the three fat-water experiments, we observed in general an *increase* in the T_1 of fat from its pure T_1 value as the fat fraction *decreased*. Conversely, the T_1 of water *decreased* from its pure T_1 value when the mixture composition became less water dominant. In the oil-water emulsion experiment, the variation in the fat and water T_1 values was significant when the mixture composition became less than 30% fat (water dominant) and 30% water (fat dominant), respectively. The use of MRS provided good separation of the different chemical

moieties in each experimental setup, as well as excellent data fits for the saturation-recovery signal equation. Based on present results, all of our hypotheses are corroborated.

The present findings reinforce the issue of T_1-bias when using fat fraction indices from chemical-shift-based methods such as IDEAL. The T_1-bias between fat (*F*) and water (*W*) spins is intuitive (11). However, the variation in component fat and water T_1 as a function of fat fraction is not obvious and further complicates the issue of fat quantification. Nonetheless, low-flip-angle approaches (8,11) that minimize T_1-bias or schemes that explicitly measure T_1 (11) to correct for the signal bias remain important in accurate fat fraction quantification. A particularly interesting conclusion can be drawn from the current results. At low fat fractions —often encountered in liver fat quantification—the component T_1 of water and fat is potentially very close in value (Fig. 3). This similarity in T_1 values actually *lessens* the degree of T_1 bias between fat and water. Consequently, the need for T_1-bias correction is less of an issue, and an Ernst angle approach could potentially be favorable. A similar argument can be made for high-fat-fraction scenarios. Figure 3 further suggests that the greatest T_1 bias between fat and water in mixture likely occurs at intermediate fat fractions.

In this work, we focused only on the T_1 of methylene fat protons. One limitation of this is that the observed change in water T_1 may be partly influenced by the olenific fat peak (5.2–5.4 ppm), which is in close proximity to the water peak. However, the acetone-water setup was not susceptible to this limitation. Previous literature has reported that other fat components (e.g., olenific, methyl, diallyic) have individual and different natural T_1 values (23,24). It can be implied that the T_1 of these minor fat peaks may also change when in mixture. Quantification of the degree of T_1 change in these minor fat peaks will require a higher magnetic field strength for greater spectral resolution.

The findings of fat T_1 variation will unlikely have any implications on conventional T_1-based fat suppression methods (short T_1/tau inversion recovery). Based on the oil-water phantom experiment (Fig. 3), pure fat had a T_1 of 314 msec. The fat T_1 did not begin to deviate substantially from its natural T_1 value until the fat fraction was less than 30%. Let M_{O_F} denote the fully relaxed longitudinal magnetization of pure fat. An inversion recovery (IR) sequence using inversion time = 218 msec that is set to null pure fat will more than adequately suppress not only pure fat but also a majority of voxels with fat-signal fractions between 30% and 100%. Consider a voxel with a 30% fat fraction, whose fully relaxed longitudinal magnetization can be denoted as $0.3 \cdot M_{O\_F}$. According to Fig. 3, the fat T_1 is 779 msec. During an IR experiment, M_Z will relax at most from $-0.3 \cdot M_{O\_F}$ to $+0.3 \cdot M_{O\_F}$. At inversion time =218 msec, $|M_Z|$ will have recovered to approximately 50% of ($0.3 \cdot M_{O\_F}$), which results in a net detectable magnetization of only 15% of M_{O_F}. For another voxel with a 10% fat fraction (fat T_1 1332 msec), the net magnetization at inversion time =218 msec is less than 7% of M_{O_F}. In terms of short T_1/tau inversion recovery fat suppression performance in clinical applications, these residual fat signals will not likely raise concerns.

We have also performed experiments using IDEAL with inversion-recovery fast spin echo and driven equilibrium single pulse observation of T_1 (25) imaging approaches in lieu of MRS to measure fat and water T_1 values in mixture (26). Comparable results and trends in T_1 were observed in phantoms and in vivo. With IDEAL-inversion-recovery fast spin echo, data were acquired as a function of inversion time. With driven equilibrium single pulse observation of T_1, data were acquired as a function of flip angle, similar to the approach used by Liu et al. (11). IDEAL-reconstructed fat and water signals were fitted to either inversion-recovery or spoiled-gradient-echo signal equations to determine component T_1 values. Confounding factors such as T_2^*, T_1 bias, multifat-peak modeling, and amplitude of radiofrequency field flip-angle nonuniformity were collectively considered for accurate IDEAL fat-water decomposition (8–11) and signal fitting. For both inversion-recovery fast spin echo and driven

equilibrium single pulse observation of T_1, a high number of signal averages (>5) were needed to ensure ample signal-to-noise ratio in the decomposed fat and water images. Physiologic constraints were also set for the T_1 estimates (11) from driven equilibrium single pulse observation of T_1 and inversion-recovery fast spin echo. These constraints were necessary based on our previous experience in estimating T_1 values from noisy signal curves at low fat and water fractions acquired with only one to two signal averages.

The oil-water phantom results from this work bear resemblance to a recent study by Sharma et al. (16), which also used MRS to measure the water and fat T_1 values, but at 1.5 T. In emulsions of 10 and 30% fat fractions, the authors found both the water and fat T_1 to decrease with increasing concentrations of oil. For the 10% mixture, the T_1 of water was measured as 821.7 msec, while in the 30% mixture, it was 591.7 msec. The T_1 of fat in the 10% mixture was 680.3 msec, while in the 30% mixture, it was a significantly lower 185.2 msec. The emulsions also contained varying concentrations of iron additives, which were used to generate differences in T_2 relaxation. Sharma et al. (16) further reported the hepatic fat T_1 in a subject with a 13% fatty liver to be 485 msec, which anecdotally seems greater than reported literature values of pure fat at 1.5 T (280–340 msec) (21,22). In another article, by Poon et al. (27), the authors performed a study at 1.5 T in thigh muscle in a patient with myositis (skeletal muscle inflammation), which is often accompanied by fatty infiltration. It was found that the fat T_1 increased from 187 to 396 msec and the water T_1 decreased from 1257 to 993 msec when the fat-signal fraction increased from 24 to 71% in several regions of interest. In constructing several homogeneous fat-water emulsions of different fat fractions with matched fat and water T_1 values at 3 T, Dyke et al. (28) reported that it was necessary to dope the water and agarose gel ingredients with varying amounts of gadolinium contrast agent to decrease the water T_1 and match it to the shorter fat T_1.

A detailed description behind the change in T_1 is beyond the scope and intent of this article, but insights can be gleaned from literature on general relaxation theory (29), relaxation behaviors in binary liquid mixtures (30), and some intuition. It is known in chemistry that when two components (A and B) are combined to form a mixture, the critical points of the solution (e.g., freezing, boiling) will consequently vary nonlinearly as a function of the concentrations of A and B present. This principle can be extended to T_1 *spin-lattice* relaxation. Fundamentally, T_1 depends on a match between the amplitude of static field–dependent Larmor frequency (f_{Larmor}) of protons in a molecule and the tumbling rate (inverse molecule correlation time) of the local molecular lattice ($f_{lattice}$) surrounding the molecule of interest. When the two are equal, T_1 relaxation is the most energy efficient, leading to a short T_1 value. This is the primary reason underlying fat's characteristic short T_1 and free water's long T_1 in physiologic MRI. The tumbling rate of a molecular lattice composed of large fat molecules is closely matched the proton Larmor frequency at 1.5 and 3 T (e.g., $f_{Larmor} \neq f_{lattice}$, therefore, short T_1). In contrast, the tumbling rate of a lattice composed of small, free-water molecules is significantly greater than the Larmor value (e.g., $f_{Larmor} = f_{lattice}$, therefore, long T_1). Therefore, it is plausible that any structural change in the lattice will lead to variations in the lattice tumbling rate and thus affect T_1.

In oil-water suspensions, it is conceivable that the structure of the molecular lattice will change as a function of the concentration of fat and water present in the lattice. At very low or high fat fractions, the dominant lattice is likely determined by the majority species. Large fatty acid moieties may aggregate into small micelles at low fat fractions when water is the dominant lattice. Conversely, they may link together to form large molecular sheets at high fat fractions where fat is the dominant lattice. Consequently, the observed T_1 spin-lattice relaxation rates of water and fat species will likely depend on the dominant lattice. This potentially explains why the T_1 values of water and fat are very close at low and high fat fractions where the dominant lattice is clearly defined by the majority species. At intermediate fat fractions where

both water and fat are present in comparable amounts, an intricate and complex lattice will likely form, giving rise to distinct water and fat T_1 values.

Consider the extreme case where a large fat molecule that is surrounded in a solvent consisting primarily of smaller water molecules (low fat fraction). Also consider in contrast the opposite extreme case where the fat molecule is surrounded in a solvent composed mostly of similar fat molecules (high fat fraction). In the low-fat-fraction environment, the increase in the number of local smaller water molecules with shorter correlation times and faster tumbling rates will lead to a $f_{lattice}$ that is greater than the proton f_{Larmor} of the fat molecule. As a result of this mismatch, the fat molecule is energetically less efficient at interacting with the water-dominant lattice. Consequently, an *increase* in fat T_1 will occur. In contrast, f_{Larmor} and $f_{lattice}$ are more closely matched for the high-fat-fraction environment (fat-dominant lattice), thereby promoting *faster T_1* relaxation. The same argument can be applied from the perspective of a water molecule. An increasing presence of larger, slow-tumbling fat molecules in the solvent within the immediate vicinity of a water molecule will decrease the local $f_{lattice}$ in comparison to that of a water-rich lattice. This will effectively bring the local $f_{lattice}$ surrounding the water molecule of interest closer to the f_{Larmor} of the water spins, thereby *lowering* the water T_1.

Applications involving fat infiltration of skeletal muscles and organs can potentially benefit from the present findings. Relationships between T_1 and muscle fiber composition have been reported (31), where it was speculated that the proportion of slow- to fast-twitch fibers, along with their relative fat contents, plays a determining role. Assessment of muscle and organ triglyceride content remains important in studies of Duchenne muscular dystrophy (32) and Gaucher's disease (33) and in metabolic disorders and the etiology of obesity (34,35). Furthermore, differences in triglyceride composition (fatty acid chain length, degree of saturation) may also influence T_1 due to molecular size and geometry.

In conclusion, this work has described the variation in T_1 of fat and water as a function mixture composition and has provided supporting evidence from MRS. It is an additional factor that falls under the complex framework of accurate fat fraction quantification in MRI and reinforces the notion that T_1 bias is a required consideration.

Acknowledgments

References

1. Ma J. Breath-hold water and fat imaging using a dual-echo two-point Dixon technique with an efficient and robust phase-correction algorithm. Magn Reson Med 2004;52:415–419. [PubMed: 15282827]

2. Reeder SB, Pineda AR, Wen Z, Shimakawa A, Yu H, Brittain JH, Gold GE, Beaulieu CH, Pelc NJ. Iterative decomposition of water and fat with echo asymmetry and least-squares estimation (IDEAL): application with fast spin-echo imaging. Magn Reson Med 2005;54:636–644. [PubMed: 16092103]

3. Xiang QS. Two-point water-fat imaging with partially-opposed-phase (POP) acquisition: an asymmetric Dixon method. Magn Reson Med 2006;56:572–584. [PubMed: 16894578]

4. Hernando D, Haldar JP, Sutton BP, Ma J, Kellman P, Liang ZP. Joint estimation of water/fat images and field inhomogeneity map. Magn Reson Med 2008;59:571–580. [PubMed: 18306409]

5. Kim H, Taksali SE, Dufour S, Befroy D, Goodman TR, Petersen KF, Shulman GI, Caprio S, Constable RT. Comparative MR study of hepatic fat quantification using single-voxel proton spectroscopy, two-point Dixon and three-point IDEAL. Magn Reson Med 2008;59:521–527. [PubMed: 18306404]

6. Kellman P, Hernando D, Shah S, Zuehlsdorff S, Jerecic R, Mancini C, Liang ZP, Arai AE. Multiecho Dixon fat and water separation method for detecting fibrofatty infiltration in the myocardium. Magn Reson Med 2009;61:215–221. [PubMed: 19097213]

7. Bornert P, Keupp J, Eggers H, Aldefeld B. Whole-body 3D water/fat resolved continuously moving table imaging. J Magn Reson Imaging 2007;25:660–665. [PubMed: 17326078]

8. Bydder M, Yokoo T, Hamilton G, Middleton MS, Chavez AD, Schwimmer JB, Lavine JE, Sirlin CB. Relaxation effects in the quantification of fat using gradient echo imaging. Magn Reson Imaging 2008;26:347–359. [PubMed: 18093781]

9. Yu H, Shimakawa A, McKenzie CA, Brodsky E, Brittain JH, Reeder SB. Multiecho water-fat separation and simultaneous R2* estimation with multifrequency fat spectrum modeling. Magn Reson Med 2008;60:1122–1134. [PubMed: 18956464]

10. Yu H, McKenzie CA, Shimakawa A, Vu AT, Brau AC, Beatty PJ, Pineda AR, Brittain JH, Reeder SB. Multiecho reconstruction for simultaneous water-fat decomposition and T2* estimation. J Magn Reson Imaging 2007;26:1153–1161. [PubMed: 17896369]

11. Liu CY, McKenzie CA, Yu H, Brittain JH, Reeder SB. Fat quantification with IDEAL gradient echo imaging: correction of bias from T1 and noise. Magn Reson Med 2007;58:354–364. [PubMed: 17654578]

12. Hu HH, Nayak KS. Quantification of absolute fat mass using an adipose tissue reference signal model. J Magn Reson Imaging 2008;28:1483–1491. [PubMed: 19025936]

13. Bottomley PA. Spatial localization in NMR spectroscopy *in vivo*. Ann N Y Acad Sci 1987;508:333–348. [PubMed: 3326459]

14. Naressi A, Couturier C, Devos JM, Janssen M, Mangeat C, de Beer R, Graveron-Demilly D. Java-based graphical user interface for the MRUI quantitation package. MAGMA 2001;12:141–152. [PubMed: 11390270]

15. Naressi A, Couturier C, Castang I, de Beer R, Graveron-Demilly D. Java-based graphical user interface for MRUI, a software package for quantitation of in vivo/medical magnetic resonance spectroscopy signals. Comput Biol Med 2001;31:269–286. [PubMed: 11334636]

16. Sharma P, Martin DR, Pineda N, Xu Q, Vos M, Anania F, Hu X. Quantitative analysis of T2-correction in single-voxel magnetic resonance spectroscopy of hepatic lipid fraction. J Magn Reson Imaging 2009;29:629–635. [PubMed: 19243059]

17. Bernard CP, Liney GP, Manton DJ, Turnbull LW, Langton CM. Comparison of fat quantification methods: a phantom study at 3.0T. J Magn Reson Imaging 2008;27:192–197. [PubMed: 18064714]

18. Cinti S. The role of brown adipose tissue in human obesity. Nutr Metab Cardiovasc Dis 2006;16:569–574. [PubMed: 17113764]

19. Hu, HH.; Smith, DL.; Nagy, TR.; Goran, MI.; Nayak, KS. Identification of brown adipose tissue in mice using IDEAL fat-water MRI. 17th Meeting of the International Society of Magnetic Resonance in Medicine; Honolulu, Hawaii. 2009. p. 210

20. Zancanaro C, Nano R, Marchioro C, Sbarbati A, Boicelli A, Osculati F. Magnetic resonance spectroscopy investigations of brown adipose tissue and isolated brown adipocytes. J Lipid Res 1994;35:2191–2199. [PubMed: 7897317]

21. de Bazelaire CM, Duhamel GD, Rofsky NM, Alsop DC. MR imaging relaxation times of abdominal and pelvic tissues measured in vivo at 3.0 T: preliminary results. Radiology 2004;230:652–659. [PubMed: 14990831]

22. Gold GE, Han E, Stainsby J, Wright G, Brittain J, Beaulieu C. Musculoskeletal MRI at 3.0 T: relaxation times and image contrast. AJR Am J Roentgenol 2004;183:343–351. [PubMed: 15269023]

23. Brix G, Heiland S, Bellemann ME, Koch T, Lorenz WJ. MR imaging of fat-containing tissues: valuation of two quantitative imaging techniques in comparison with localized proton spectroscopy. Magn Reson Imaging 1993;11:977–991. [PubMed: 8231682]

24. Ren J, Dimitrov I, Sherry AD, Malloy CR. Composition of adipose tissue and marrow fat in humans by H NMR at 7 tesla. J Lipid Res 2008;49:2055–2062. [PubMed: 18509197]

25. Deoni SC, Rutt BK, Peters TM. Rapid combined T1 and T2 mapping using gradient recalled acquisition in the steady state. Magn Reson Med 2003;49:515–526. [PubMed: 12594755]

26. Hu, HH.; Sung, K.; Nayak, KS. Apparent change in the T1 of lipids in mixture. 17th Meeting of the International Society of Magnetic Resonance in Medicine; Honolulu, Hawaii. 2009. p. 4448

27. Poon CS, Szumowski J, Plewes DB, Ashby P, Henkelman RM. Fat/water quantitation and differential relaxation time measurement using chemical shift imaging technique. Magn Reson Imaging 1989;7:369–382. [PubMed: 2811618]

28. Dyke, JP.; Lauto, A.; Schneider, E.; Matei, C.; Borja, J.; Mao, X.; Shungu, DC.; Jakubowski, A.; Lis, E.; Ballon, D. Homogeneous water-lipid phantoms with matched T1 and T2 relaxation times for quantitative magnetic resonance imaging of tissue composition at 3.0 tesla. 12th Meeting of the International Society of Magnetic Resonance in Medicine; Kyoto, Japan. 2004. p. 2212

29. Cowan, B. Nuclear magnetic resonance and relaxation. Cambridge: Cambridge University Press; 1997. p. 458

30. Ragozzino E, Bortone C. Proton spin-lattice relaxation in binary liquid mixtures: determination of the mixed translational contributions. Mol Phys 1971;22:525–533.

31. Houmard JA, Smith R, Jendrasiak GL. Relationship between MRI relaxation time and muscle fiber composition. J Appl Physiol 1995;78:807–809. [PubMed: 7775322]

32. Wren TA, Bluml S, Tseng-Ong L, Gilsanz V. Three-point technique of fat quantification of muscle tissue as a marker of disease progression in Duchenne muscular dystrophy: preliminary study. AJR Am J Roentgenol 2008;190:W8–12. [PubMed: 18094282]

33. Terk MR, Dardashti S, Liebman HA. Bone marrow response in treated patients with Gaucher disease: evaluation by T1-weighted magnetic resonance images and correlation with reduction in liver and spleen volume. Skeletal Radiol 2000;29:563–571. [PubMed: 11127678]

34. Sinha R, Dufour S, Petersen KF, LeBon V, Enoksson S, Ma YZ, Savoye M, Rothman DL, Shulman GI, Caprio S. Assessment of skeletal muscle triglyceride content by (1)H nuclear magnetic resonance spectroscopy in lean and obese adolescents: relationships to insulin sensitivity, total body fat, and central adiposity. Diabetes 2002;51:1022–1027. [PubMed: 11916921]

35. Goodpaster BH, Wolf D. Skeletal muscle lipid accumulation in obesity, insulin resistance, and type 2 diabetes. Pediatr Diabetes 2004;5:219–226. [PubMed: 15601366]
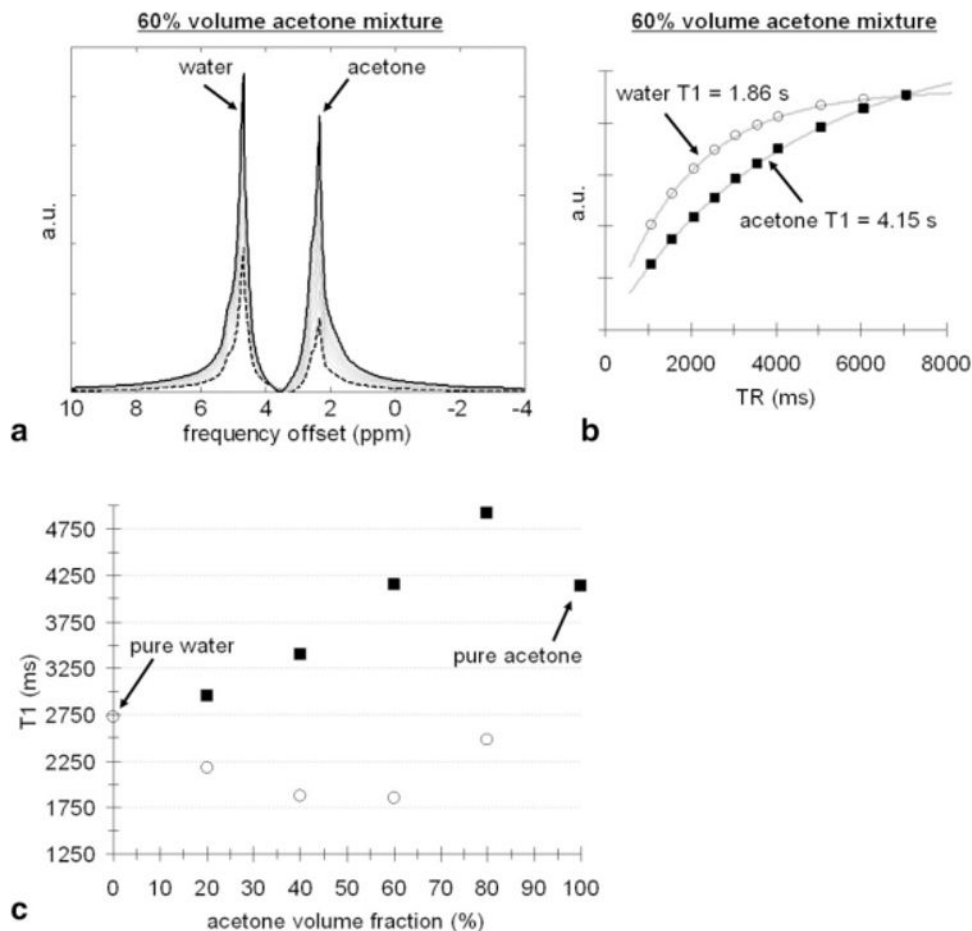
FIG. 1.
Results from acetone-water mixtures. **a:** Raw, unprocessed MRS spectra from the 60% acetone mixture. A spectrum obtained with a TR of 7070 msec is shown in solid black. A spectrum obtained with a TR of 1070 msec is shown in dashed black. **b:** Plot of spectral signal as a function of TR for acetone (black square) and water (open circle) components with saturation-recovery fitted curves. **c:** Plot of acetone and water T_1 as a function of mixture composition, demonstrating evident changes of T_1 in mixture from pure values.
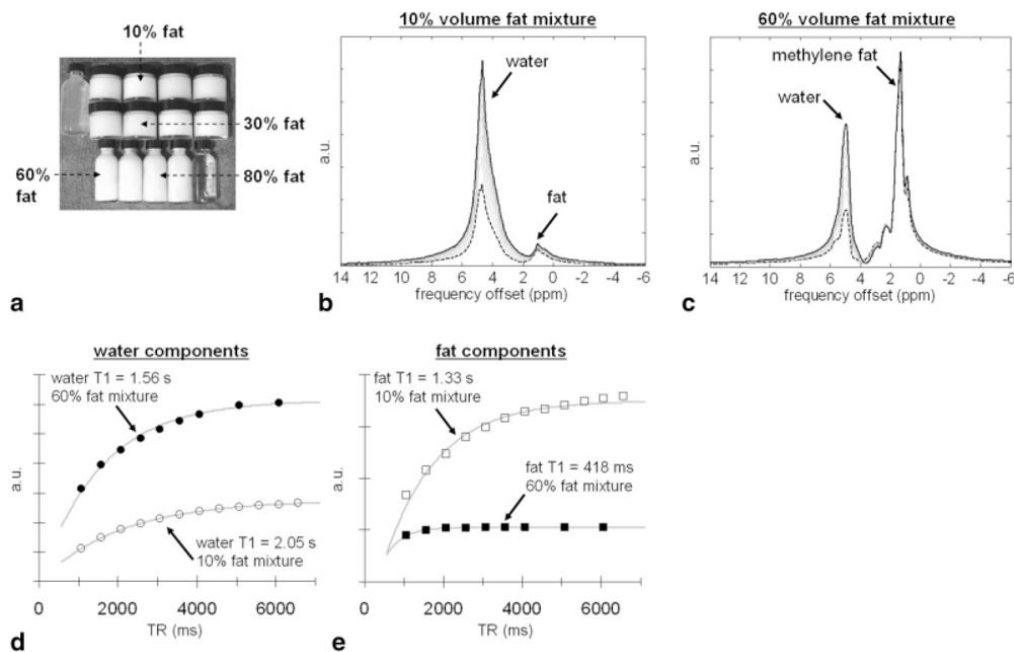
FIG. 2.
Results from oil-water emulsions. **a:** Photograph of the emulsions. Clear white liquid on the upper left is water and agar. Clear liquid on the lower right is vegetable (corn oil). **b,c:** Raw, unprocessed MRS spectra from 10 and 60% fat mixtures for various TR values (long TR, solid black; short TR, dashed black, respectively). **d,e:** Plots of spectral signal as a function of TR for water (circles) and fat (squares) components, respectively, along with fitted curves. Note evident differences in T_1 values.
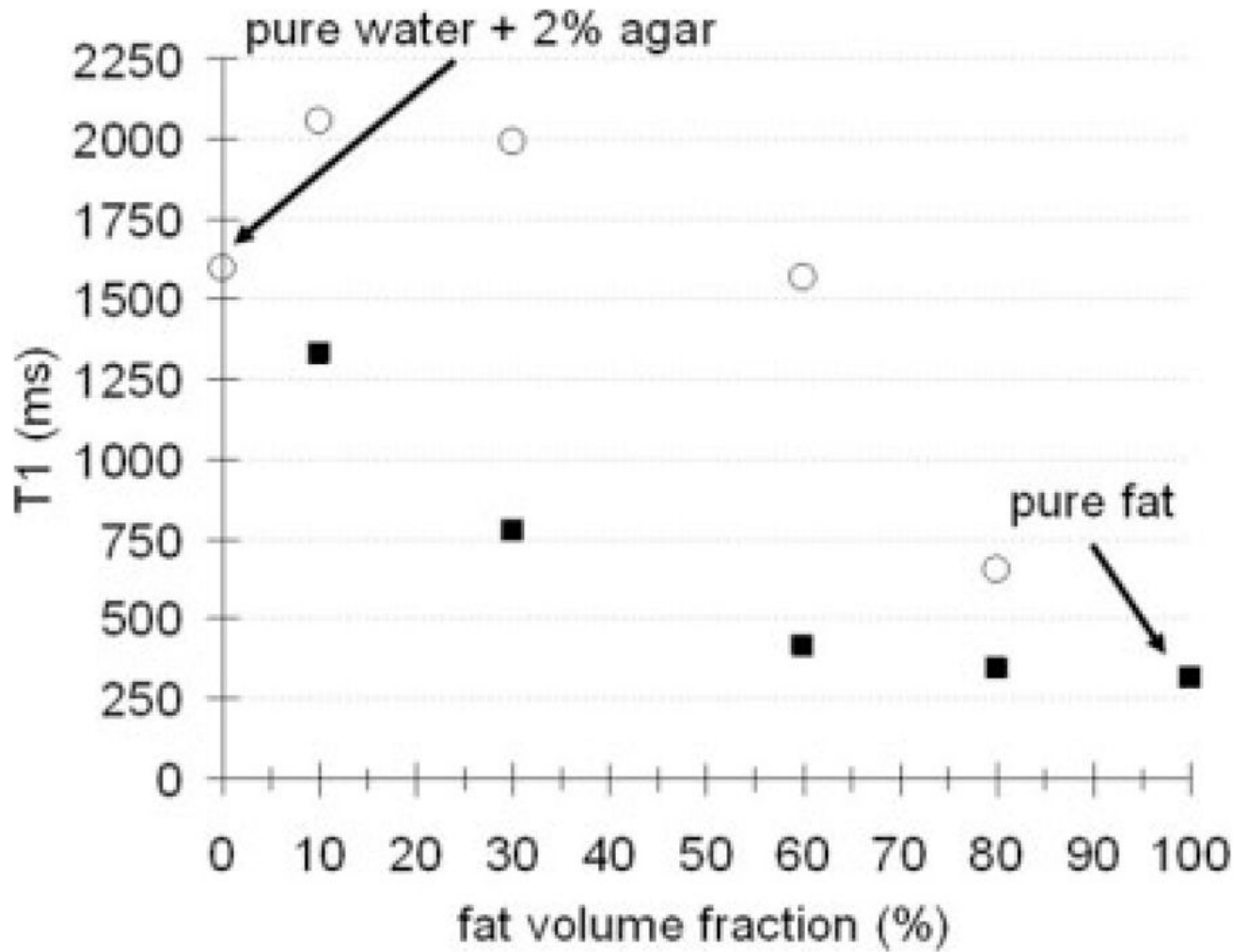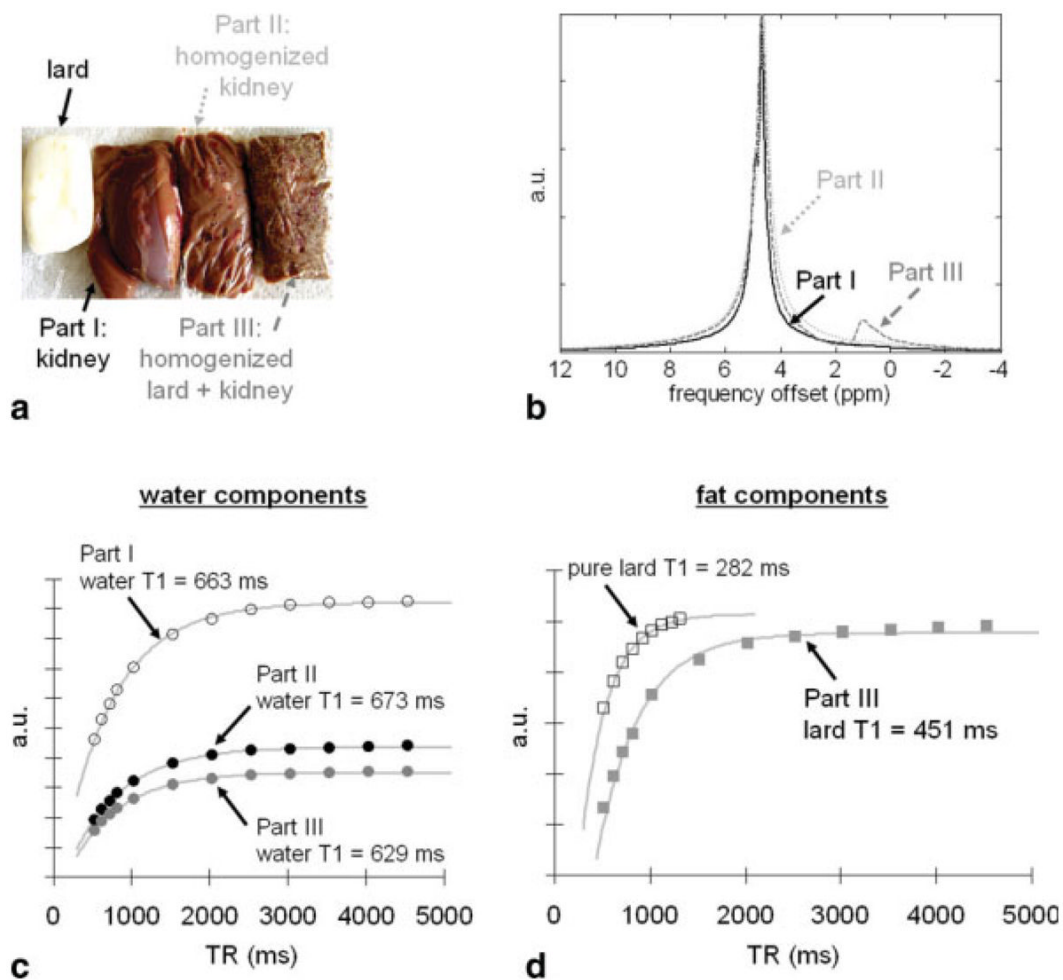
FIG. 3.
Overall result from oil-water emulsions. Plot of fat (black squares) and water (open circles)
T_1 as a function of fat fraction. The change in the T_1 of both moieties from their pure values
when in relatively homogeneous emulsions is evident.

FIG. 4.
Results from kidney-lard mixtures. **a:** Photograph of lard (white) and the three-part samples.
b: Corresponding MRS spectra. Part III has a fat fraction of approximately 16%. **c:** Spectral
signal plots as a function of TR for the water component in parts I-III. Homogenizing the tissues
(part II) does not appear to affect the T_1 of the water component in comparison to reference
intact kidney tissue (part I). **d:** Spectral signal plots for the lard component in part III and in
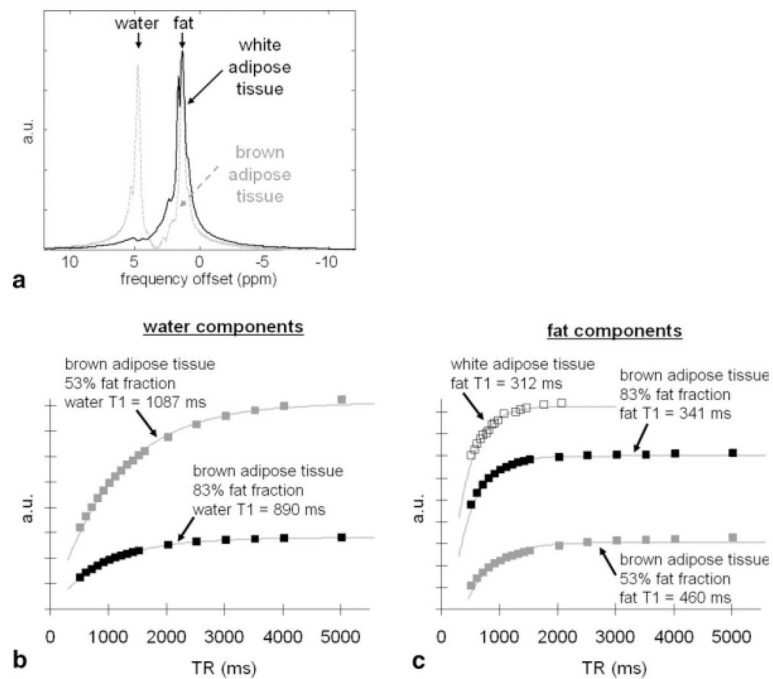pure lard, demonstrating a near 170-msec (37%) difference in the measured lard T_1.

FIG. 5.
Results from white and brown adipose tissue. **a:** MRS spectra of the two tissue types, demonstrating that white adipose tissue (solid black) is composed nearly entirely of lipids (1.3 ppm) while brown adipose tissue (dashed gray) contains appreciable water signals (4.7 ppm). **b:** Spectral signal plots of the water component as a function of TR, showing slight differences in water T_1 for two samples of brown adipose tissue with different fat content. **c:** Corresponding plots of the fat component, showing more pronounced differences in the fat T_1 from that of pure white adipose tissue.

Table 1

List of TR Values Used in Each Spectroscopy Experiment

Experiment	Figure number	TR (ms)
Acetone-water	1	1070, 1570, 2070, 2570, 3070, 3570, 4070, 5070, 6070, 7070
Oil-water	2, 3	Emulsions
		1070, 1570, 2070, 2570, 3070, 3570, 4070, 4570, 5070, 5570, 6070, 6570
		Pure oil
		550, 620, 720, 820, 920, 1020, 1120, 1220, 1320
Kidney-lard	4	Mixtures
		525, 625, 725, 825, 1025, 1525, 2025, 2525, 3025, 3525, 4025, 4525
		Pure lard
		525, 625, 725, 825, 925, 1025, 1125, 1225, 1325,
Brown and white adipose tissue	5	Brown
		525, 625, 725, 825, 925, 1025, 1125, 1225, 1325, 1425, 1525, 1625, 2025, 2525, 3025,
		3525, 4025, 5025
		White
		525, 575, 625, 675, 725, 775, 825, 875, 925, 975, 1075, 1275, 1375, 1475, 1775, 2075